
Line integral convolution-based non-local structure tensor

Yuhui Zheng* and Kai Ma

School of Computer and Software,
Nanjing University of Information Science and Technology,
No. 219, Ning Liu Road, Pukou District, 210044 Nanjing, China
Email: zhengyh@vip.126.com
Email: 1300424427@qq.com
*Corresponding author

Shunfeng Wang and Jing Sun

Binjiang College,
Nanjing University of Information Science and Technology,
No. 219, Ning Liu Road, Pukou District, 210044 Nanjing, China
Email: wsfnuist@126.com
Email: tisingh@163.com

Jianwei Zhang

College of Math and Statistics,
Nanjing University of Information Science and Technology,
No. 219, Ning Liu Road, Pukou District, 210044 Nanjing, China
Email: zhangjw@nuist.edu.cn

Abstract: The non-local structure tensors have received much attention recently. However, the current computation methods of non-local structure tensor fail to fully use the anisotropic characteristic of tensors, hence resulting in limited performance. To address this problem, we present a novel anisotropic non-local regularisation scheme that integrates the atomic decomposition strategy with an extended line integral convolution method using non-local means filtering technique, in order to sufficiently utilise the spatial direction relevancy of tensors for their anisotropic smoothing. Experimental results on the test images show that our proposed anisotropic non-local structure tensor is superior to the current representative nonlinear structure tensors in corner detection.

Keywords: non-local structure tensor; image structure analysis; tensor field regularisation.

Reference to this paper should be made as follows: Zheng, Y., Ma, K., Wang, S., Sun, J. and Zhang, J. (2018) 'Line integral convolution-based non-local structure tensor', *Int. J. Computational Science and Engineering*, Vol. 16, No. 1, pp.98–105.

Biographical notes: Yuhui Zheng received his PhD degree in the Nanjing University of Science and Technology, China in 2009. Currently, he is an Associate Professor in the School of Computer and Software, Nanjing University of Information Science and technology. His research interests cover image processing, pattern recognition, and remote sensing information system.

Ma Kai received her BS degree in Computer and Software from Nanjing University of Information Science and Technology (NUIST), China in 2016. Currently, she is a postgraduate in the College of Computer and Software, NUIST. His research interests cover image processing and pattern recognition.

Shunfeng Wang is a Professor at the Binjiang College, Nanjing University of Information Science and Technology. His research interests cover pattern recognition, artificial intelligence, and medicine image processing.

Jing Sun received her PhD degree in the Nanjing University of Science and Technology, China in 2013. Currently, she is an Associate Professor in the Binjiang College, Nanjing University of Information Science and technology. Her research interests cover information security, image processing, and intelligent computing.

Jianwei Zhang received his PhD degree in the Nanjing University of Science and Technology, China in 2006. Currently, he is a Professor at the College of Mathematics and Physics, Nanjing University of Information Science and Technology. His research interests cover pattern recognition, artificial intelligence, and remote sensing information processing.

This paper is a revised and expanded version of a paper entitled ‘Atomic decomposition based anisotropic non-local structure tensor’ presented at IEEE International Conference on Image Processing (ICIP), Québec, Canada, 27–30 September 2015.

1 Introduction

As a useful tool for image orientation and geometric structure analysis, the structure tensor simultaneously introduced by Bigün et al. (1991) and Förstner and Gulch (1987) has been successfully applied in many fields of computer vision and image processing, including feature detection (Köthe, 2003; Zhang et al., 2009), optic flow computation (Nagel and Gehrke, 1998; Middendorf and Nagel, 2001), orientation extraction (Brox et al., 2006; Andersson and Duchkov, 2003), image magnification (Lefkimiatis et al., 2015), image restoration (Hahn and Lee, 2009; Li et al., 2017; Estellers et al., 2015), image segmentation (de Luis-Garcia et al., 2008; Han et al., 2009), etc. In these applications, analysis accuracy and robustness to noise are its key requirements.

In the early low-level computer vision field, image gradients were frequently utilised for image content analysis. However, straight application of image gradient often suffers from the robustness problem, especially in the presence of noise. Intuitively, one can average the image gradients within a local neighbourhood or window with a low-pass filter to suppress noise. Nevertheless, this usually results in cancellation effect (Brox et al., 2006) when image gradients with opposite directions to each other appear in the calculation windows. Such effect can be avoided by using the structure tensor that is a smoothed version of second-moment matrix (called tensor hereinafter) of an image. In general, the tensor is a 2×2 symmetric positive semi-definite matrix computed by the outer product of image gradient. The structure tensor can be viewed as a symmetric positive definite matrix, owing to its integration of the local or non-local knowledge about image orientations and contents.

The classical structure tensor, also named as linear structure tensor (LST), applies linear regularisation technique to smooth the tensor field. Although linear filtering is robust to noise, it tends to distort important geometric information embedded in the tensors. To address this drawback, various adaptive local structure tensors (ALSTs) have been proposed with the aid of the nonlinear regularisation techniques. For instance, Nagel and Gehrke (1998) utilised an adaptive Gaussian kernel to regularise the tensor field for optic flow calculation, which was further extended by Middendorf in the works of Middendorf and Nagel (2001, 2002). Van den Boomgaard and van de Weijer (2002) proposed an ALST through robust statistics to extract image orientation. Köthe (2003) introduced a nonlinear structure tensor via utilising an hour-glass shaped

filter to adaptively smooth the tensor field. Brox et al. (2006) presented an ALST construction framework by means of typical nonlinear diffusion equation such as the total variation (TV) type for the applications of image feature detection, optic flow estimation and image denoising. Hahn and Lee (2009) suggested a diffusion equation-based tensor regularisation method with a modified diffusivity matrix, which is composed of the first derivatives of an image instead of the derivatives of the tensor. Though the existing ALSTs have shown their effectiveness in many application fields, they fail to discriminate image details that differ only in scale.

To overcome this problem, several multi-scale nonlinear structure tensors (MNSTs) have been introduced through incorporating scale knowledge into tensor field regularisation. For example, Scheunders (2006) proposed a MNST for image fusion and enhancement by means of image multi-resolution decomposition using discrete wavelet transform (Mallat and Zhong, 1992; Mallat, 1999), which are followed by an extension in Han et al. (2009) to texture image segmentation. Zhang et al. (2009) presented a MNST with a multi-scale bilateral filtering for image corners detection. It should be noted that these tensor regularisation approaches are localised, in the sense that merely the spatially neighbouring related information is involved in the structure tensor constructions. Recently, Doré et al. (2007) presented a NLST by extending the non-local means filtering (NLMF) (Buades et al., 2005; Zhang et al., 2016) to the tensor field. Lefkimiatis and Osher (2015) employed the NLST to design regularisation operator to address image processing tasks. Chierchia et al. (2014) and Zheng et al. (2015a) used the non-local TV regularisations (Giboa and Osher, 2009; Lou et al., 2010) to construct structure tensors for image recovery and adaptively selecting the regularisation parameters, respectively. In these cases, the Euclidean distance is commonly employed for the similarity computation of the tensors. Because the Euclidean distance inaccurately measures the similarity of matrix-valued data, the existing NLSTs still have limited performance. Moreover, they are calculated in an isotropic way.

Zheng et al. (2015b) presented an anisotropic non-local structure tensor (ANST) by utilising a decomposition and reconstruction scheme. In this work, the tensor field regularisation can be reformulated into a problem of multiple vector-fields regularisation, thereby avoiding employment of Euclidean distance to evaluate the similarity of tensors. Nevertheless, this ANST computation probably

induces reconstruction errors, because of the discrete implementation of the structure tensor reconstruction. To overcome the problem, we attempt to explore a new way to obtain ANST by utilising the tensor direction decomposition strategy without reconstruction. A novel ANST construction method is introduced through jointing tensor direction decomposition with a variation of the traditional line integral convolution (LIC) (Cabral and Leedom, 1993).

The remainder of this paper is organised as follows. Section 2 briefly describes the theoretical aspects of the structure tensor and the LIC computation. Details of our proposed ANST construction method are presented in Section 3. The experimental results are given in Section 4. Finally, Section 5 concludes the work.

2 Preliminaries

This section briefly introduces the basic theoretical background of the structure tensor and the traditional LIC.

2.1 Structure Tensor and its eigendecomposition

Let I denote an image with a bounded domain Ω . The structure tensor S of image I can be defined as:

$$S = \varphi(J = \nabla I \nabla I^T) = \varphi \begin{pmatrix} I_x I_x & I_x I_y \\ I_x I_y & I_y I_y \end{pmatrix} = \varphi \begin{pmatrix} t_1 & t_2 \\ t_2 & t_3 \end{pmatrix}, \quad (1)$$

where J is the tensor, $\nabla I = (I_x, I_y)^T$ denotes the image gradient, T is the transpose, and $\varphi(\bullet)$ stands for the tensor regularising operator. Generally, in the nonlinear structure tensor construction a small-scale Gaussian smoothing is carried out before the adaptive regularisation operator $\varphi(\bullet)$ to suppress noise. Hence, the nonlinear structure tensors calculation can be uniformly written as:

$$S = \varphi \left(\mathbf{g}_\rho * \begin{pmatrix} t_1 & t_2 \\ t_2 & t_3 \end{pmatrix} \right) = \begin{pmatrix} s_1 & s_2 \\ s_2 & s_3 \end{pmatrix} \quad (2)$$

where $*$ denotes the convolution operator and \mathbf{g}_ρ stands for the Gaussian kernel with standard deviation ρ . In (2), the Gaussian-smoothed structure tensor \hat{J} is accomplished by convolving tensor J component-wisely using the Gaussian kernel \mathbf{g}_ρ as follows:

$$\hat{J} = \mathbf{g}_\rho * \begin{pmatrix} t_1 & t_2 \\ t_2 & t_3 \end{pmatrix} = \begin{pmatrix} \mathbf{g}_\rho * t_1 & \mathbf{g}_\rho * t_2 \\ \mathbf{g}_\rho * t_2 & \mathbf{g}_\rho * t_3 \end{pmatrix} \quad (3)$$

The two eigenvalues of structure tensor S , i.e., λ_1 and λ_2 , and the corresponding orthogonal eigenvectors γ_1 and γ_2 can be respectively computed by:

$$(s_1 + s_3 \pm \sqrt{(s_1 - s_3)^2 + 4(s_2)^2}) \geq \lambda_2 \quad (4)$$

$$\gamma_1 = \begin{bmatrix} 2s_2 \\ s_3 - s_1 + \sqrt{(s_1 - s_3)^2 + 4(s_2)^2} \end{bmatrix} \quad (5)$$

$$\gamma_2 = \begin{bmatrix} s_3 - s_1 + \sqrt{(s_1 - s_3)^2 + 4(s_2)^2} \\ -2s_2 \end{bmatrix} \quad (6)$$

With the eigenvalues and the eigenvectors, the spectral decomposition formula of S can be written as:

$$S = \lambda_1 \gamma_1 \gamma_1^T + \lambda_2 \gamma_2 \gamma_2^T \quad (7)$$

In principle, the eigenvector γ_2 determines the dominant orientation of image structure, and different image geometric contents including flat areas, edges and corners can be discriminated with a combined use of the eigenvalues-based measures, such as the magnitude $\lambda_1 + \lambda_2$ and the coherence $\sqrt{\lambda_1 - \lambda_2}$. Generally, the values of magnitude measure and the coherence measure are both small in image flat areas. At image edges, the two measure values are both large, while image corners have large magnitude measure value but small coherence measure value.

2.2 Traditional LIC

For visual representation of vector fields, LIC was first proposed by Cabral and Leedom (1993) and then have been extensively studied and widely extended (Tschumperlé, 2005; Falk and Weiskopf, 2008). The main idea of LIC is to smooth an image (only containing noise) through averaging the pixels along an integral curve with respect to a given vector field. The continuous formulation of LIC calculation can be written as (Cabral and Leedom, 1993):

$$I_q^{LIC} = \frac{1}{Z} \int_{-p}^p \phi(\tau) I(\ell_{(q,\tau)}^w) d\tau \quad (8)$$

$$Z = \int_{-p}^p \phi(\tau) d\tau \quad (9)$$

where $\phi(\bullet)$ is a 1-dimensional even function that is usually the Gaussian function, ℓ^w denotes an integral curve related to the vector field w , which starts from the point q and parameterised by the parameter τ , the parameter p also named as length-factor determines the size of integral curve, and Z is the normalising factor. See Cabral and Leedom (1993) and Tschumperlé (2005) for the integral curve acquirement and computation in details. Note that the classical LIC is used for smoothing image pixels. In this paper we attempt to extend it to regularise the tensor field.

3 Proposed ANST

Let us recall two types of popular diffusion partial differential equations with divergence form, which are given as follows:

$$I_t = \text{div}(\psi(\|\nabla I\|)\nabla I) \quad (10)$$

$$I_t = \text{div}(D\nabla I) \quad (11)$$

where I_t denotes the derivative of the image I with respect to the time t , $\text{div}(\bullet)$ stands for the divergence operator, $\psi(\bullet)$ is a scalar-valued function of the gradient magnitude and defines the locally smoothing scale, and D is named as the diffusion tensor steering the diffusion process. Usually, the calculation of diffusion tensor D relies on the structure tensor and can be accomplished by:

$$D = f_1(\lambda_1, \lambda_2) \gamma_2 \gamma_2^T + f_2(\lambda_1, \lambda_2) \gamma_1 \gamma_1^T = \begin{pmatrix} d_1 & d_2 \\ d_2 & d_3 \end{pmatrix} \quad (12)$$

To construct our proposed ANST, we begin with directionally projecting all the diffusion tensors onto different orientations ranging from 0 to π , which leads to the atomic vector fields (AVFs) as follows:

$$w_i^\theta = D_i \quad V_\theta = \begin{pmatrix} d_1^i \cos \theta + d_2^i \sin \theta \\ d_2^i \cos \theta + d_3^i \sin \theta \end{pmatrix} \quad (13)$$

$$\theta = k\pi/M, \quad k = 0 \dots M-1 \quad (14)$$

where M denotes the number of projection directions. Then, for current point, a set of integral curves $\hat{h}_i = (\ell_i^{w^\theta})_{\theta=0}^\pi$ can be achieved from the AVFs. Within \hat{h}_i each integral curve $\ell_i^{w^\theta}$ with length of $2p + 1$ is calculated from its corresponding AVF W^θ , by means of tracking forward and backward from current point i with a simple and efficient approach based on the Runge-Kutta integration algorithm (Cabral and Leedom, 1993), which has been successfully used for image regularisation. For other interesting integration technique, we refer to the work in Zhao et al. (2016). In fact, integral curves can express the nonlocal behaviour of AVFs and their calculation is based on the spatial direction related image regularities distributed into the AVFs, including the continuity and the coherency. Therefore, they can be utilised to adaptively concatenate direction relevant tensors for subsequent smoothing.

With the integral curve $\ell_i^{w^\theta}$, a curve-level tensor regularisation can be carried out firstly. To do so, we present a tensor version of the LIC (T-LIC) based on integral curve $\ell_i^{w^\theta}$, which is calculated as

$$\hat{S}_{i,\theta}^{LIC} = \frac{1}{\hat{Z}_i^\theta} \int_{-p}^p \hat{\phi}_\theta(i, \tau) \hat{J}(\ell_{i,\tau}^{w^\theta}) d\tau \quad (15)$$

where the normalising factor \hat{Z}_i^θ is defined by

$$\hat{Z}_i^\theta = \int_{-p}^p \hat{\phi}_\theta(i, \tau) d\tau \quad (16)$$

In implementation, the corresponding discrete formulas of (15) and (16) are given by

$$S_{i,\theta}^{LIC} = \frac{1}{Z_i^\theta} \sum_{\tau=-p}^p \phi_\theta(i, \tau) \hat{J}(\ell_{i,\tau}^{w^\theta}) \quad (17)$$

$$Z_i^\theta = \sum_{\tau=-p}^p \phi_\theta(i, \tau) \quad (18)$$

Compared to the traditional LIC computation that employs the pixel-wise filtering operator on image, here we utilise a ‘1-dimensional’ NLMF, that is $\phi_\theta^{NL}(\bullet)$, to replace the function $\phi_\theta(\bullet)$ in (17) and (18), which regularises the Gaussian smoothed tensors along integral curve $\ell_i^{w^\theta}$ as follows:

$$\phi_\theta^{NL}(i, \tau) = \exp\left(-\frac{\|\hat{J}(\mathcal{F}_i^l) - \hat{J}\mathcal{F}_\tau^l\|_{g_\varepsilon}^2}{\Upsilon}\right) \quad (19)$$

where $\hat{J}(\mathcal{F}_i^l)$ denotes a set of Gaussian-smoothed tensors in square region \mathcal{F}_i^l centred at i , with size of $l \times l$, $\|\bullet\|_{g_\varepsilon}^2$ is the Euclidean distance weighted by a Gaussian function with zero mean and standard deviation ε , and the controlling parameter Υ is calculated here by:

$$\Upsilon = \beta |\hat{J}(\mathcal{F}_i^l)| \sigma^2 \quad (20)$$

where $|\hat{J}(\mathcal{F}_i^l)| = l^2$ stands for the size of set $\hat{J}(\mathcal{F}_i^l)$, σ denotes the standard deviation of image noise, and the parameter β is set manually. The usage of the extended NLMF is based on two considerations: non-local behaviour of the integral curves, and better robustness of the multipoint method to noise and outliers than the traditional point-wise approach. Normally, Euclidean metric would yield inaccurate estimation, and theoretically the Riemannian metrics would be more appropriate for the similarity measure of tensor data. However, the computation in the Riemannian framework comes at the cost of high time consumption because of its usual implementation in an iterative way. Encouragingly, the tensors on the integral curves are spatial direction related. As a result, the Euclidean distance-based measurement can be viewed as a good estimation for the similarity of tensors concatenated by the related integral curve.

Using the curve-level smoothed tensor, a planar-level (full) tensor regularisation is carried out by averaging all the results of T-LICs achieved with the multiple integral curves, hence leading to the LIC-ANST. The continuous and discrete formulas for LIC-ANST calculation are respectively given by:

$$\hat{S}_o^{LIC} = \frac{1}{\pi} \int_{\theta=0}^\pi \frac{1}{\hat{Z}_i^\theta} \int_{-p}^p \hat{\phi}_\theta^{NL}(i, \tau) \hat{J}(\ell_{i,\tau}^{w^\theta}) d\tau d\theta \quad (21)$$

$$S_o^{LIC} = \frac{1}{M} \sum_{\theta=0}^\Theta \frac{1}{Z_i^\theta} \sum_{\tau=-p}^p \phi_\theta^{NL}(i, \tau) \hat{J}(\ell_{i,\tau}^{w^\theta}) \quad (22)$$

where Θ denotes the maximum projection orientation, computed by (14). In (21) and (22), the tensor regularisation is driven by the multiple integral curves that adaptively capture non-local spatial direction related tensors in a non-local way. Each integral curve depicts the image

regularity in a certain direction. Because of the introduction of spatial directional correlations into tensor field regularisation, the construction of LICANST is anisotropic.

4 Experimental results

In the experiments, our proposed structure tensors are compared with five representative structure tensors, that is the TV type diffusion equation-based ALST (TV-ALST) (Brox et al., 2006), the NLST (Doré et al., 2007), the non-local TV regularisation-based NLST (TV-NLST) (Zheng et al., 2015a), and the tensor decomposition and reconstruction-based ANST (TDRANST) (Zheng et al.,

2015b), in corner feature detection (Zhao et al., 2016; Zhang et al., 2016). Three test images shown in Figure 1 are used for corner detection, including the artificial image, the lab image and the House image. The corners are detected by jointly using two eigenvalue-based measures, i.e., the magnitude $\lambda_1 + \lambda_2$ and the coherence $\sqrt{\lambda_1 - \lambda_2}$. The ground-truth corners are obtained by averaging five manually labelling results independently conducted by five students. In addition, we mainly utilise three quantitative indexes for result evaluation, that is the correct recognition rate (CRR), the false recognition rate (FRR) and the mean localisation error (MLE).

Figure 1 Original test images and their corresponding ground-truth corners (see online version for colours)

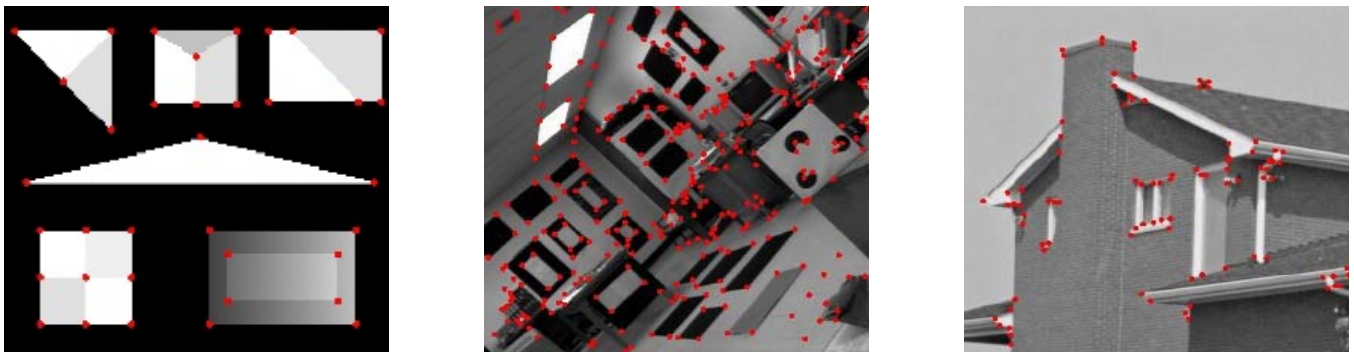


Figure 2 Corner detection results on noisy artificial image, (a) noisy image (b) TV-ALST (c) NLST (d) TV-NLST (e) TDR-ANST (f) LIC-ANST (see online version for colours)

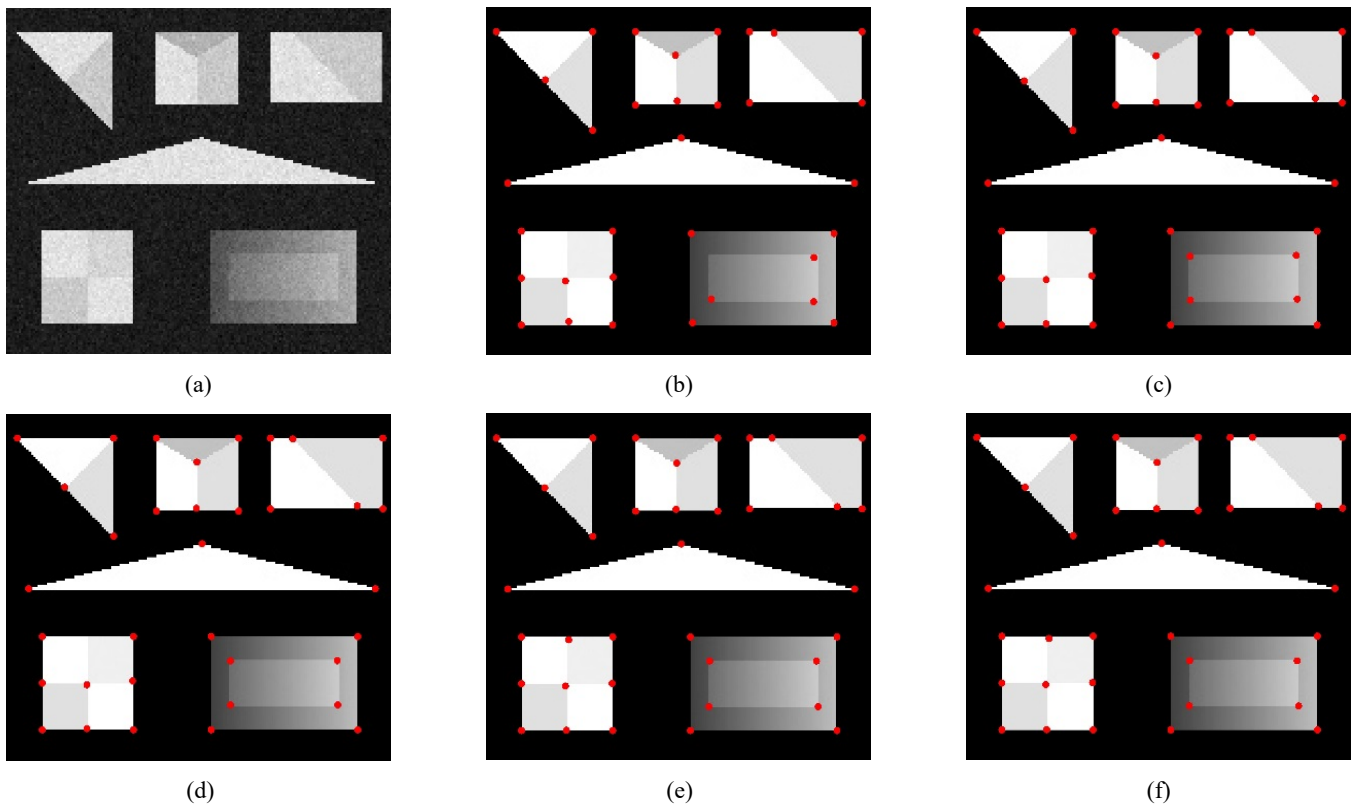


Figure 3 Corner detection results on noisy house image, (a) noisy image (b) TV-ALST (c) NLST (d) TV-NLST (e) TDR-ANST (f) LIC-ANST (see online version for colours)

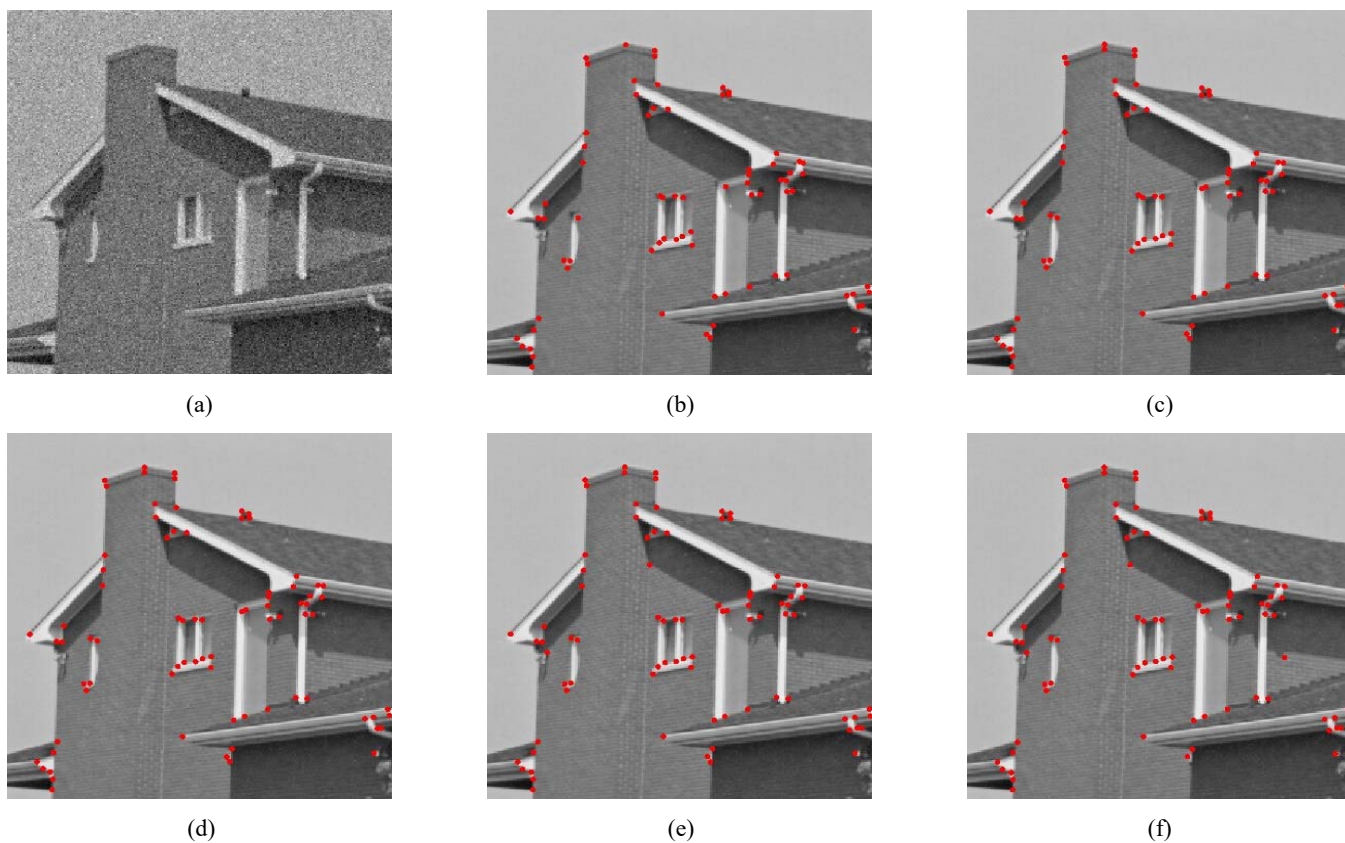


Figure 4 Corner detection results on noisy lab image, (a) noisy image (b) TV-ALST (c) NLST (d) TV-NLST (e) TDR-ANST (f) LIC-ANST (see online version for colours)

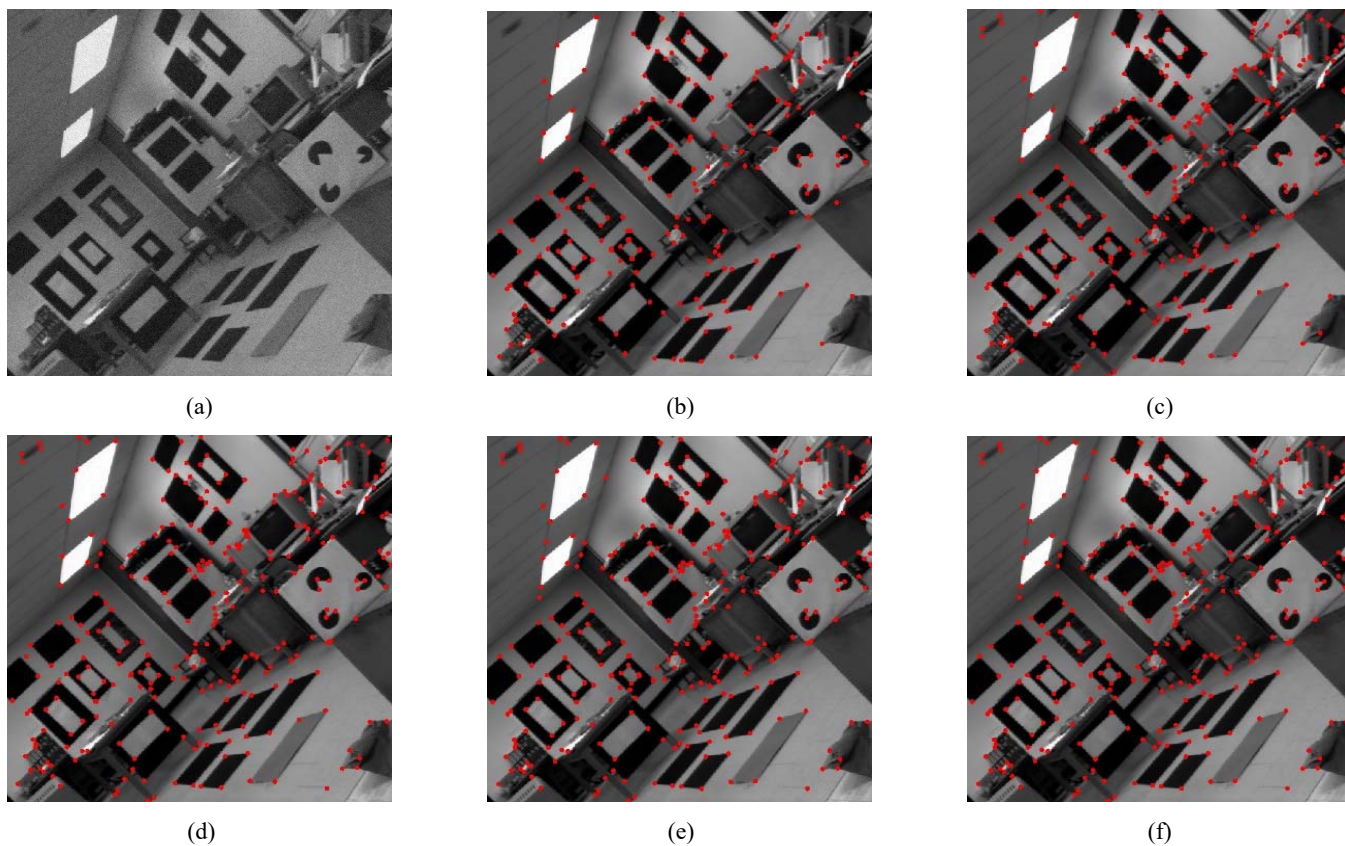


Figure 2 illustrates the corner-detecting results on the noisy artificial image Figure 2(a), which is generated by adding the Gaussian noise ($\sigma^2 = 25$) into the original image shown in Figure 1. Figures 2(b) to 2(h) display the corner detection results given by the five nonlinear structure tensors. We can clearly see from Figure 2 that the ALST (TV-ALST) and the isotropic NLSTs (NLST and TV-NLST) lose corners in the low-contrast and critically degraded areas, whereas the anisotropic NLSTs, including TDR-ANST and LIC-ANST, detect all corners from the noisy image. Visually, relative to TDR-ANST, we can observe that LIC-ANST performs well in term of corner localisation accuracy, especially in poor quality image regions.

Table 1 Comparison of corner detection results

<i>Image</i>	<i>Method</i>	<i>Detected corners</i>	<i>CRR (%)</i>	<i>FRR (%)</i>	<i>MLE (pixels)</i>
Artificial image	TV-ALST	33	91.67	0.000	1.2121
	NLST	35	97.22	0.000	0.8571
	TV-NLST	35	97.22	0.000	0.7143
	TDRANST	36	100.0	0.000	0.5278
	LIC-ANST	36	100.0	0.000	0.5000
House image	TV-ALST	78	81.72	2.564	2.421
	NLST	81	84.95	2.469	1.392
	TV-NLST	83	86.02	3.614	1.200
	TDR-ANST	85	88.17	3.529	0.976
	LIC-ANST	86	88.17	4.651	0.854
Lab image	TV-ALST	269	85.39	2.230	1.909
	NLST	289	91.23	2.768	1.199
	TV-NLST	297	93.18	3.367	0.895
	TDR-ANST	304	95.45	3.289	0.609
	LIC-ANST	308	96.43	3.571	0.572

Figure 3 compares the detection results of the seven structure tensors on the noisy house image with Gaussian noise level $\sigma^2 = 20$. As seen in Figures 3(b) to 3(e), the two isotropic NLSTs can extract corners from the low-contrast noisy chimney top, which is mainly attributed to the non-local smoothing methodology attempting to discover more similar tensors within the whole support domain for boosting tensor regularisation. Compared to the artificial image, the house image contains more similar corners. Hence, the NLSTs (both the isotropic and the anisotropic) can detect corners even in the low quality areas. However, from Figures 3(d) to 3(f) we can see that the TDR-ANST has limited corner-detecting performance in seriously corrupt image areas. Our proposed ANST is able to yield relatively better corner estimation results, which is verified again by the experiment on the noisy corner-rich lab image shown on Figure 4. In Figure 4, the lab image is corrupted by the Gaussian noise with variance $\sigma^2 = 15$, shown in Figure 4(a). For further performance assessment of the ANST, see Table 1 for details.

Table 1 presents a quantitative comparison of the corner-detecting results of all experiments. We can see that

the our proposed structure tensor yields relatively good results as a whole, achieving a better trade-off than the CRR, the MLE and the FRR.

5 Conclusions

In this work, a new ANST, that is LIC-ANST, has been introduced through a new scheme of combining the direction projection-based tensor decomposition and the TLICs, which consists of the following three core stages:

- 1 direction composition and integral curve acquirement
- 2 T-LIC calculation to curve-level tensor regularisation
- 3 ANST construction by means of the average of the T-LIC results.

In implementation, relative to four representative nonlinear structure tensors including the LAST and the NLSTs, our proposed ANST performs well in complex image corner detection.

Acknowledgements

This work was partly supported by the National Natural Science Foundation of China under Grants 61402235 and 61672295, the Natural Science Foundation of the Higher Education Institutions of Jiangsu Province under Grant 14KJD520004, and the PAPD (a project funded by the priority academic program development of Jiangsu Higher Education Institutions).

References

- Andersson, F. and Duchkov, A.A. (2003) ‘Extended structure tensors for multiple directionality estimation’, *Geophys. Prospect*, Vol. 60, No.6, pp.1135–1149.
- Bigün, J., Granlund, G.H. and Wiklund, J. (1991) ‘Multidimensional orientation estimation with applications to texture analysis and optical flow’, *IEEE Trans. Pattern Anal. Mach. Intell.*, Vol. 13, No. 8, pp.775–790.
- Brox, T., Weickert, J., Burgeth, B. and Mrázek, P. (2006) ‘Nonlinear structure tensors’, *Image Vis. Comput.*, Vol. 24, No. 1, pp.41–55.
- Buades, A., Coll, B. and Morel, J.M. (2005) ‘A non-local algorithm for image denoising’, *CVPR*, San Diego, CA, USA June.
- Cabral, B. and Leedom, L.C. (1993) ‘Imaging vector fields using line integral convolution’, *GIGGRAPH CGUT*, New York, USA.
- Chierchia, G., Pustelnik, N., Pesquet-Popescu, B. and Pesquet, J-C. (2014) ‘A non-local structure tensor based approach for multicomponent image recovery problems’, *IEEE Trans. Image Process.*, December, Vol. 23, No. 12, pp.5531–5544.
- de Luis-Garcia, R., Deriche, R. and Alberola-Lopez, C. (2008) ‘Texture and color segmentation based on the combined use of the structure tensor and the image components’, *Signal Process.*, April, Vol. 88, No. 4, pp.776–795.

- Doré, V., Moghaddam, R.F. and Cheriet, M. (2007) 'Non-local adaptive structure tensors: application to anisotropic diffusion and shock filtering', *Image Vis. Comput.*, November, Vol. 29, No. 11, pp.730–743.
- Estellers, V., Soatto, S. and Bresson, X. (2015) 'Adaptive regularization with the structure tensor', *IEEE Trans. Image Process.*, Vol. 24, No. 6, pp.1777–1790.
- Falk, M. and Weiskopf, D. (2008) 'Output-sensitive 3D line integral convolution', *IEEE Trans. Vis. Comput. Gr.*, April, Vol. 14, No. 4, pp.820–834.
- Förstner, W. and Gulch, E. (1987) 'A fast operator for detection and precise location of distinct points, corners and centres of circular features', *ISPRS*, Interlaken, Swiss.
- Giboa, G. and Osher, S. (2009) 'Nonlocal operators with application to image processing', *Multiscale Model. Simul.*, Vol. 7, No. 3, pp.1055–1028.
- Hahn, J. and Lee, C. (2009) 'A nonlinear structure tensor with the diffusivity matrix composed of the image gradient', *J. Math Imaging Vis.*, Vol. 34, No. 2, pp.137–151.
- Han, S., Tao, W., Wang, D., Tai, X-C. and Wu, X. (2009) 'Image segmentation based on GrabCut framework integrating multiscale nonlinear structure tensor', *IEEE Trans. Image Process.*, October, Vol. 18, No. 10, pp.2289–2302.
- Köthe, U. (2003) 'Edge and junction detection with an improved structure tensor', *Pattern Recognition, Lecture Notes in Computer Science*, Vol. 2781, pp.25–32.
- Lefkimiatis, S. and Osher, S. (2015) 'Nonlocal structure tensor functionals for image regularization', *IEEE Trans. Computational Imaging.*, March, Vol. 1, No. 1, pp.16–29.
- Lefkimiatis, S., Roussos, A., Maragos, P., Maragos, P. and Unser, M. (2015) 'Structure tensor total variation', *SIAM J. Imag. Sci.*, May, Vol. 8, No. 2, pp.1090–1122.
- Li, W., Wang, B., Zou, J. and Shen, J. (2017) 'A collaborative filtering recommendation method based on TagIEA expert degree model', *Int. J. Computational Science and Engineering*, June, Vol. 14, No. 4, pp.321–329.
- Lou, Y., Zhang, X., Osher, S. and Bertozzi, A. (2010) 'Image recovery via nonlocal operators', *J. Sci. Comput.*, Vol. 42, No. 2, pp.185–197.
- Mallat, S. (1999) *A Wavelet Tour of Signal Processing*, 2nd ed., Academic, New York.
- Mallat, S. and Zhong, S. (1992) 'Characterization of signals from multiscale edges', *IEEE Trans. Pattern Anal. Mach. Intell.*, Vol. 14, pp.710–732.
- Middendorf, M. and Nagel, H-H. (2001) 'Estimation and interpretation of discontinuities in optical flow fields', *ICCV*, Vancouver, Canada.
- Middendorf, M. and Nagel, H-H. (2002) 'Empirically, convergent adaptive estimation of grayvalue structure tensor', in Van Gool, L. (Ed.): *Pattern Recognition, Lecture Notes in Computer Science*, Vol. 2449, Springer, Berlin.
- Nagel, H.H. and Gehrke, A. (1998) 'Spatiotemporally adaptive estimation and segmentation of OF-fields', *ECCV*, Freiburg, Germany.
- Scheunders, P. (2002) 'A multivalued image wavelet representation based on multiscale fundamental forms', *IEEE Trans. Image Process.*, May, Vol. 11, No. 5, pp.568–575.
- Tschumperlé, D. (2005) 'LIC-based regularization of multi-valued images', *ICIP*, Québec, Canada.
- van den Boomgaard, R. and van de Weijer, J. (2002) 'Robust estimation of orientation for texture analysis', *Pro. Second International Workshop on Texture Analysis and Synthesis*, Copenhagen.
- Zhang, D., Han, J., Li, C., Wang, J. and Li, X. (2016) 'Detection of co-salient objects by looking deep and wide', *International Journal of Computer Vision*, November, Vol. 120, No. 2, pp.215–232.
- Zhang, D., Zhao, Y. and Du, M. (2016) 'A novel supervised feature extraction algorithm: enhanced within-class linear discriminant analysis', *Int. J. Computational Science and Engineering*, July, Vol. 13, No. 1, pp.12–23.
- Zhang, L., Zhang, L. and Zhang, D. (2009) 'A multi-scale bilateral structure tensor based corner detector', *ACCV*, Xi'an, China.
- Zhao, Y., Ding, D.Z. and Chen, R.S. (2016) 'A discontinuous Galerkin time domain integral equation method for electromagnetic scattering from PEC objects', *IEEE Trans. Antennas Propag.*, June, Vol. 64, No. 6, pp.2410–2417.
- Zheng, Y., Beon, J., Zhang, W. and Chen, Y. (2015a) 'Adaptively determining regularization parameters in nonlocal total variation regularization for image denoising', *Electron. Lett.*, January, Vol. 51, No. 2, pp.144–145.
- Zheng, Y., Zhou, X., Jeon, B., Sun, Q. and Wu, Y. (2015b) 'Atomic decomposition based anisotropic non-local structure tensor', *ICIP*, Québec, Canada.